2-(1*H*-2-Benzimidazolyl)-6-(1-(arylimino)ethyl)pyridyl Iron(II) and Cobalt(II) Dichlorides: Syntheses, Characterizations, and Catalytic Behaviors toward Ethylene Reactivity

Liwei Xiao,[†,‡] Rong Gao,[‡] Min Zhang,[‡] Yan Li,[‡] Xiaoping Cao,*[,†] and Wen-Hua Sun*[,†,‡]

State Key Laboratory of Applied Organic Chemistry, College of Chemistry and Chemical Engineering, Lanzhou University, Lanzhou 730000, People's Republic of China, and Key Laboratory of Engineering Plastics, Beijing National Laboratory for Molecular Sciences, Institute of Chemistry, Chinese Academy of Sciences, Beijing 100190, People's Republic of China

Received December 1, 2008

A series of tridentate N^N^N iron(II) and cobalt(II) dichloride complexes bearing 2-(1*H*-2-benzimidazolyl)-6-(1-(arylimino)ethyl)pyridines were synthesized and characterized by elemental and spectroscopic analyses. Single-crystal X-ray diffraction studies of representative examples of the cobalt and iron complexes confirm distorted bipyramidal geometry around the metal center. Upon coordination of a methanol solvent molecule, a geometry change to distorted octahedral was observed. The steric and electronic effects on catalytic activity are evaluated for different substituents in the arylimino part of the ligand: Me, Et, ^{i}Pr, Cl, and Br in *ortho*- and Me and H in *para*-position. On treatment with methylaluminoxane (MAO) or modified MAO (MMAO), the iron(II) complexes exhibited good activities of up to 10^6 g·mol^{-1}(Fe)·h^{-1} for ethylene oligomerization and moderate activities for polymerization, while cobalt(II) complexes showed moderate activities for ethylene dimerization. The best activities were observed with iron complexes with bulky ^{i}Pr groups in the aryl moiety. In comparison to the analogues containing the 2-(1-alkyl-2-benzimidazolyl)-6-(1-(arylimino)ethyl)pyridines, the iron complexes bearing 2-(1*H*-2-benzimidazolyl)-6-(1-(arylimino)ethyl)pyridines showed the best activity toward ethylene reactivity.

1. Introduction

α-Olefins have been extensively used as substrates for preparing detergents, lubricants, plasticizers, and oil field chemicals, or as monomers for copolymers, etc. Driven by academic and industrial considerations of the important process of ethylene oligomerization for α-olefins, efficient catalysts and catalytic processes are pursued for high catalytic activity and selectivity for the formation of linear α-olefins. Over the past decade, progress has been made in ethylene reactivity (polymerization and oligomerization) by late transition metal complex catalysts.[1−5] Regarding iron and cobalt systems, 2,6-bis(imino)pyridines, initially discovered by the groups of Brookhart and Gibson individually, are well known.[6−9] There are many works on modifying 2,6-bis(imino)pyridyl metal complexes;[1−3,10,11] however, few reports showed alternative models for iron catalysts with catalytic activity from considerable[12] to high.[13] Beyond the works on derivatizations of 2,6-bis(imino)pyridine iron catalysts,[14] we have intensively explored alternative models of iron complex catalysts for ethylene reactivity[15] through designing novel organic compounds as ligands with tridentate N^N^N coordination features such as 2-imino-1,10-phenanthrolines (**A**),[16−19] 2-(benzimidazol-2-yl)-1,10-phenanthrolines (**B**),[20,21] 2-oxazoline-1,10- phenanthrolines (**C**),[21] 2-quinoxalinyl-6-iminopyridines (**D**),[22] 2-(benzimida-

* To whom correspondence should be addressed. Tel: +86 10 62557955. Fax: +86 10 62618239. E-mail: whsun@iccas.ac.cn.
† Lanzhou University.
‡ Institute of Chemistry, Chinese Academy of Sciences.

(1) Gibson, V. C.; Spitzmesser, S. K. *Chem. Rev.* **2003**, *103*, 283.
(2) Britovsek, G. J. P.; Gibson, V. C.; Wass, D. F. *Angew. Chem., Int. Ed.* **1999**, *38*, 428.
(3) Ittel, S. D.; Johnson, L. K.; Brookhart, M. *Chem. Rev.* **2000**, *100*, 1169.
(4) Mecking, S. *Angew. Chem., Int. Ed.* **2001**, *40*, 534.
(5) Park, S.; Han, Y.; Kim, S. K.; Lee, J.; Kim, H. K.; Do, Y. *J. Organomet. Chem.* **2004**, *689*, 4263.
(6) Small, B. L.; Brookhart, M.; Bennett, A. M. A. *J. Am. Chem. Soc.* **1998**, *120*, 4049.
(7) Small, B. L.; Brookhart, M. *Macromolecules* **1999**, *32*, 2120.
(8) Britovsek, G. J. P.; Gibson, V. C.; Kimberley, B. S.; Maddox, P. J.; McTavish, S. J.; Solan, G. A.; White, A. J. P.; Williams, D. J. *Chem. Commun.* **1998**, 849.
(9) Britovsek, G. J. P.; Mastroianni, S.; Solan, G. A.; Baugh, S. P. D.; Redshaw, C.; Gibson, V. C.; White, A. J. P.; Williams, D. J.; Elsegood, M. R. J. *Chem.−Eur. J.* **2000**, *6*, 2221.
(10) Bianchini, C.; Giambastiani, G.; Rios, I. G.; Mantovani, G.; Meli, A.; Segarra, A. M. *Coord. Chem. Rev.* **2006**, *250*, 1391.
(11) Gibson, V. C.; Redshaw, C.; Solan, G. A. *Chem. Rev.* **2007**, *107*, 1745.
(12) (a) Britovsek, G. J. P.; Gibson, V. C.; Hoarau, O. D.; Spitzmesser, S. K.; White, A. J. P.; Williams, D. J. *Inorg. Chem.* **2003**, *42*, 3454. (b) Britovsek, G. J. P.; Baugh, S. P. D.; Hoarau, O.; Gibson, V. C.; Wass, D. F.; White, A. J. P.; Williams, D. J. *Inorg. Chim. Acta* **2003**, *345*, 279.
(13) Small, B. L.; Rios, R.; Fernandez, E. R.; Carney, M. J. *Organometallics* **2007**, *26*, 1744.
(14) Ma, Z.; Sun, W.-H.; Li, Z.-L.; Shao, C.-X.; Hu, Y.-L.; Li, X.-H. *Polym. Int.* **2002**, *51*, 994.
(15) Sun, W.-H.; Zhang, S.; Zuo, W. C. R. *Chim.* **2008**, *11*, 307.
(16) Wang, L.; Sun, W.-H.; Han, L.; Yang, H.; Hu, Y.; Jin, X. *J. Organomet. Chem.* **2002**, *658*, 62.
(17) Sun, W.-H.; Jie, S.; Zhang, S.; Zhang, W.; Song, Y.; Ma, H.; Chen, J.; Wedeking, K.; Fröhlich, R. *Organometallics* **2006**, *25*, 666.
(18) Jie, S.; Zhang, S.; Sun, W.-H.; Kuang, X.; Liu, T.; Guo, J. *J. Mol. Catal. A: Chem.* **2007**, *269*, 85.
(19) Jie, S.; Zhang, S.; Sun, W.-H. *Eur. J. Inorg. Chem.* **2007**, 5584.
(20) Zhang, M.; Hao, P.; Zuo, W.; Jie, S.; Sun, W.-H. *J. Organomet. Chem.* **2008**, *693*, 483.
(21) Zhang, M.; Gao, R.; Hao, X.; Sun, W.-H. *J. Organomet. Chem.* **2008**, *693*, 3865.

10.1021/om801141n CCC: $40.75
Publication on Web 03/06/2009

Scheme 1. Model Catalysts

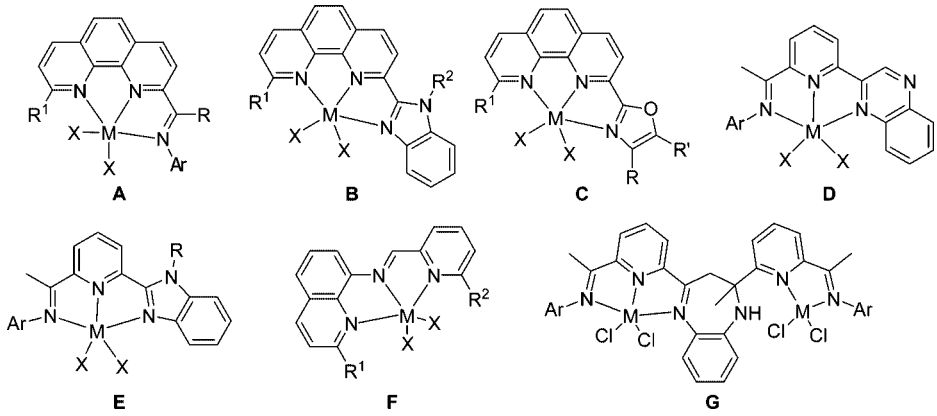

zolyl)- 6-iminopyridines (**E**),[23,24] *N*-((pyridin-2-yl)methylene)-quinolin-8-amine (**F**),[25] and 2-methyl-2,4-bis(6-iminopyridin-2-yl)-1*H*-1,5-benzodiazepines (**G**).[26,27] Those ligands were also used for their cobalt and nickel complexes as catalysts toward ethylene reactivity such as models **A**,[19,28,29] **B** and **C**,[20,21,30] **D**,[22,31] **E**,[23,24,32] **F**,[25,33] and **G**[26,27] along with their chromium complexes.[34−36] In general, iron complex catalysts not only show high catalytic activities but also produce oligomers and polyethylenes of high linearity with terminal vinyl groups. Therefore, it would be promising to explore the properties of these iron complexes in ethylene oligomerization.

Comparing synthetic procedures for the preparation of the compounds above and their catalytic performance toward activity and linearity of the resultant oligomers, model catalysts **A**[16−19] and **E**[23,24] are the most interesting; both models showed high activity, while model **E** gave higher selectivity for α-olefins. Observed in type **B** catalyst,[20] the incorporation of an alkyl group (R^2) on the N atom of the benzimidazole resulted in a decrease of oligomerization activity. This trend was also observed with 2,6-bis(2-benzimidazolyl)pyridine chromium catalysts.[37] Back to model catalyst **E** (Scheme 2), the ligands with a remaining N−H group on the benzimidazole are especially promising. Based on our previous work in obtaining diethyl 2,6-bis(β-keto-carboxylate)pyridine,[38] a new synthetic methodology toward 2-acetyl-6-(1*H*-2-benzimidazolyl)pyridine is developed with the reaction of diethyl 2,6-bis(β-keto-carboxylate)pyridine with *o*-phenylenediamine.

Scheme 2. Modification of Model Catalyst E

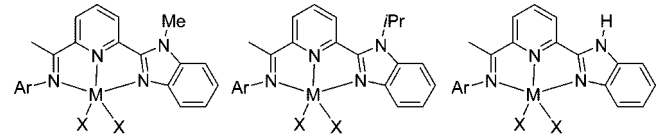

Therefore we describe the synthesis of 2-acetyl-6-(1*H*-2-benzimidazolyl)pyridine and 2-(1*H*-2-benzimidazolyl)-6-(1-(arylimino)ethyl)pyridine ligands, the preparation of the related iron and cobalt complexes, and their performance as catalysts in ethylene reactivity.

2. Results and Discussion

2.1. Syntheses of 2-Acetyl-6-(1*H*-2-benzimidazolyl)pyridine. The preparation of 6-(2-benzimidazolyl)-2-acetylpyridine from 2-(carboethoxy)-6-(2-benzimidazolyl) was successful after the benzimidazole was protected through alkylation.[23,24,32] In the process of forming an acetyl from a carboethoxy group, the ethyl β-keto-carboxylate intermediate was isolated,[38] and 2,6-bis(ethyl β-keto-carboxylate)pyridine was isolated in high yield. The reaction of 2,6-bis(ethyl β-keto-carboxylate)pyridine with *o*-phenylenediamine gave 2-acetyl-6-(1*H*-2-benzimidazolyl)pyridine in considerable 21% isolated yield. Besides 2-acetyl-6-(1*H*-2-benzimidazolyl)pyridine, the reaction intermediate, ethyl 6-(1*H*-benzmidazol-2-yl)pyridine-2-carboxylate, was isolated in 29% yield. These two organic compounds were confirmed by ^{1}H NMR, ^{13}C NMR, FT-IR spectroscopy, and elemental analyses.

2.2. Syntheses of 2-(1*H*-Benzimidazolyl)-6-(1-arylimino-ethyl)pyridines and the Title Complexes. The condensation reaction of 2-(1*H*-benzimidazolyl)-6-acetylpyridine with substituted anilines routinely formed 2-(1*H*-benzimidazolyl)-6-(1-aryliminoethyl)pyridines (**L1**−**L6**) in high yields (Scheme 4), which were characterized and confirmed by ^{1}H NMR, ^{13}C NMR, and FT-IR spectra and elemental analyses. These new 2-(1*H*-benzimidazolyl)-6-(1-aryliminoethyl)pyridines acted as tridentate ligands by forming iron(II) (**Fe1**−**Fe6**) and cobalt(II) (**Co1**−**Co6**) complexes (Scheme 4).

(22) Sun, W.-H.; Hao, P.; Li, G.; Zhang, S.; Wang, W.; Yi, J.; Asma, M.; Tang, N. *J. Organomet. Chem.* **2007**, *692*, 4506.
(23) Sun, W.-H.; Hao, P.; Zhang, S.; Shi, Q.; Zuo, W.; Tang, X.; Lu, X. *Organometallics* **2007**, *26*, 2720.
(24) Chen, Y.; Hao, P.; Zuo, W.; Gao, K.; Sun, W.-H. *J. Organomet. Chem.* **2008**, *693*, 1829.
(25) Wang, K.; Wedeking, K.; Zuo, W.; Zhang, D.; Sun, W.-H. *J. Organomet. Chem.* **2008**, *693*, 1073.
(26) Zhang, S.; Vystorop, I.; Tang, Z.; Sun, W.-H. *Organometallics* **2007**, *26*, 2456.
(27) Zhang, S.; Sun, W.-H.; Kuang, X.; Vystorop, I.; Yi, J. *J. Organomet. Chem.* **2007**, *692*, 5307.
(28) Jie, S.; Zhang, S.; Wedeking, K.; Zhang, W.; Ma, H.; Lu, X.; Deng, Y.; Sun, W.-H. *C. R. Chim.* **2006**, *9*, 1500.
(29) Sun, W.-H.; Zhang, S.; Jie, S.; Zhang, W.; Li, Y.; Ma, H.; Chen, J.; Wedeking, K.; Fröhlich, R. *J. Organomet. Chem.* **2006**, *691*, 4196.
(30) Zhang, M.; Zhang, S.; Hao, P.; Jie, S.; Sun, W.-H.; Li, P.; Lu, X. *Eur. J. Inorg. Chem.* **2007**, 3816.
(31) Adewuyi, S.; Li, G.; Zhang, S.; Wang, W.; Hao, P.; Sun, W.-H.; Tang, N.; Yi, J. *J. Organomet. Chem.* **2007**, *692*, 3532.
(32) Hao, P.; Zhang, S.; Sun, W.-H.; Shi, Q.; Adewuyi, S.; Lu, X.; Li, P. *Organometallics* **2007**, *26*, 2439.
(33) Sun, W.-H.; Wang, K.; Wedeking, K.; Zhang, D.; Zhang, S.; Cai, J.; Li, Y. *Organometallics* **2007**, *26*, 4781.
(34) Zhang, S.; Jie, S.; Shi, Q.; Sun, W.-H. *J. Mol. Catal. A: Chem.* **2007**, *276*, 174.
(35) Amolegbe, S. A.; Asma, M.; Zhang, M.; Li, G.; Sun, W.-H. *Aust. J. Chem.* **2008**, *61*, 397.
(36) Chen, Y.; Zuo, W.; Hao, P.; Zhang, S.; Gao, K.; Sun, W.-H. *J. Organomet. Chem.* **2008**, *693*, 750.
(37) Zhang, W.; Sun, W.-H.; Zhang, S.; Hou, J.; Wedeking, K.; Schultz, S.; Fröhlich, R.; Song, H. *Organometallics* **2006**, *25*, 1961.
(38) Asma, M.; Adewuyi, S.; Kuang, X.; Badshah, A.; Sun, W.-H. *Lett. Org. Chem.* **2008**, *5*, 296.

Scheme 3. Synthesis of 2-Acetyl-6-(1*H*-2-benzimidazolyl)-pyridine

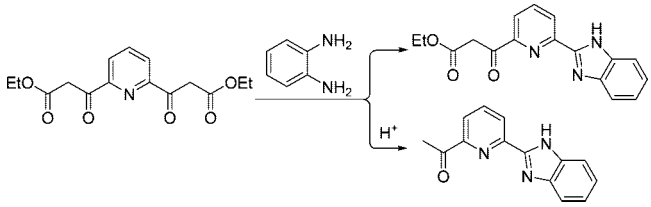

Scheme 4. Syntheses of Ligands and Title Complexes

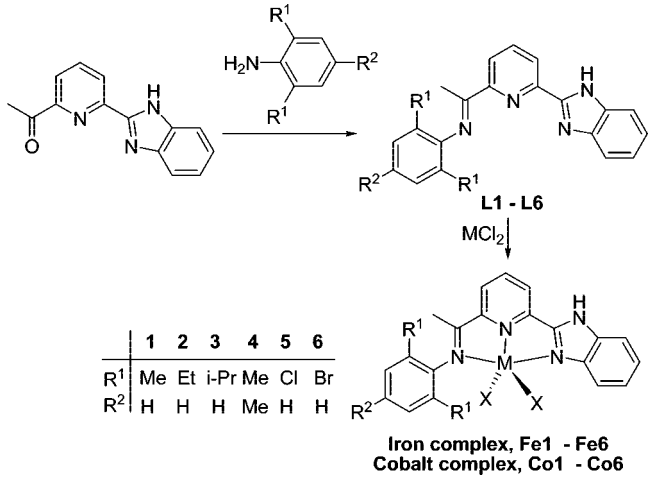

The iron(II) complexes **Fe1**−**Fe6** were prepared by mixing the corresponding ligands with 1 equiv of $FeCl_2 \cdot 4H_2O$ in ethanol under nitrogen atmosphere at room temperature (Scheme 4). The complexes were precipitated from the reaction solution as blue powders, separated by filtration, washed with diethyl ether, dried under vacuum, and isolated as air-stable compounds in good purity and high yields (80−95%). Using the same synthetic procedure, the cobalt analogues (**Co1**−**Co6**) were successfully prepared as green powders in good to high yields (Scheme 4). All metal complexes were characterized by FT−IR spectra and elemental analyses. According to the FT-IR spectra, the stretching vibration bands of the C═N groups apparently shifted to lower wavenumber with intensity greatly reduced for iron(II) complexes in the range 1595−1599 cm^{-1} and for cobalt(II) complexes in the range 1598−1600 cm^{-1} in comparison with the corresponding free ligands (1648−1655 cm^{-1}), which indicated the effective coordination between the imino group and cationic metal. The molecular structures of **Fe3**, **Co2**, and **Co4** were determined by single-crystal X-ray diffraction analyses. The iron complex **Fe3** and cobalt complex **Co2** display distorted bipyramidal geometry, whereas cobalt complex **Co4** has a distorted octahedral geometry.

2.3. Molecular Structures. Single crystals of complex **Fe3** suitable for X-ray diffraction analysis were obtained by slow diffusion of diethyl ether into a methanol solution under a nitrogen atmosphere. The coordination geometry around the iron center can be described as a distorted trigonal bipyramid (Figure 1), in which one nitrogen atom, N(2), of the pyridyl ring and two chlorine atoms (Cl(1), Cl(2)) form the equatorial plane, and the iron atom lies 0.0234 Å out of the equatorial plane. The axial planes occupied by N(1)−Fe(1)−N(3) show bond angles of 145.80(8)°. The benzimidazole ring is perpendicular to the equatorial plane and the 2,6-diisopropylphenyl group with dihedral angles of 87.9° and 84.4°. Selected bond lengths and angles are listed in Table 1. A similar geometry was also observed in other iron(II) complexes ligated by 2-(1-methyl-benzimidazolyl)-6-iminopyridines,[23] 2-(1-isopropylbenzimidazolyl)-6-iminopyridines,[24] 2-imino-1,10-phenanthrolines,[16,17] and 2-(benzimidazolyl)-1,10-phenanthrolines.[20] Moreover, the cobalt complex **Co2** also displays a distorted bipyramidal geometry.

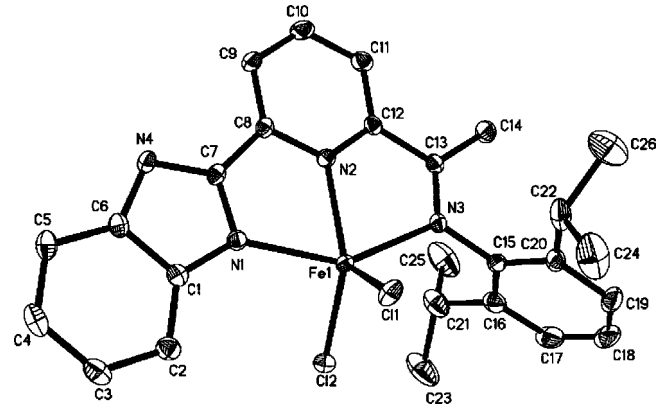

Figure 1. ORTEP drawing of complex **Fe3** with thermal ellipsoids at 30% probability. Hydrogen atoms have been omitted for clarity.

Table 1. Selected Bond Lengths (Å) and Angles (deg) for Fe3 and Co2

	Fe3	Co2
	Bond Lengths	
M(1)−N(1)	2.164(2)	2.138(2)
M(1)−N(2)	2.157(2)	2.065(2)
M(1)−N(3)	2.259(2)	2.276(3)
M(1)−Cl(1)	2.351 (1)	2.262(1)
M(1)−Cl(2)	2.2812(9)	2.295(1)
N(1)−C(7)	1.323(3)	1.323(4)
N(4)−C(7)	1.356(4)	1.359(4)
N(3)−C(13)	1.286(3)	1.281(4)
	Bond Angles	
N(1)−M(1)−N(2)	73.89(9)	76.56(10)
N(1)−M(1)−N(3)	145.80(8)	150.44(9)
N(2)−M(1)−N(3)	71.94(9)	73.97(10)
N(1)−M(1)−Cl(1)	95.83(7)	98.20(7)
N(2)−M(1)−Cl(1)	119.85(7)	121.69(8)
N(3)−M(1)−Cl(1)	102.25(7)	99.05(7)
Cl(1)−M(1)−Cl(2)	106.86(3)	113.12(4)
N(1)−M(1)−Cl(2)	98.12(7)	95.06(7)
N(2)−M(1)−Cl(2)	119.85(7)	125.17(7)
N(3)−M(1)−Cl(2)	103.93(7)	99.97(8)

Single crystals of complex **Co2** suitable for X-ray diffraction analysis were obtained by slow diffusion of diethyl ether into a DMF solution. Selected bond lengths and angles are listed in Table 1, and its molecular structure is shown in Figure 2. One nitrogen atom, N(2), of pyridine ring and two chlorine atoms (Cl(1), Cl(2)) form the equatorial plane, and the cobalt atom lies slightly out of the equatorial plane by 0.0072 Å. The other two nitrogens (N(1), N(3)) combined with the cobalt center form the axial planes occupied with bond angles of 150.44(9)°, which form a dihedral angle of 88.7° with the equatorial plane. The pyridine plane is coplanar with the benzimidazole plane with a dihedral angle of 4.2°. A similar geometry is commonly found in their cobalt(II) analogues ligated by 2-(1-methyl-benzimidazolyl)-6-iminopyridines,[23] 2-(1-isopropylbenzimidazolyl)-6-iminopyridines,[24] 2-imino-1,10-phenanthrolines,[16,28] and 2-(benzimidazolyl)-1,10-phenanthrolines.[20,21]

Single crystals of cobalt complex **Co4** suitable for X-ray diffraction analysis were obtained by slow diffusion of diethyl ether into the methanol solution. Different from the above complexes **Fe3** and **Co2**, the six-coordinated molecular structure of **Co4** forms a distorted octahedral coordination geometry

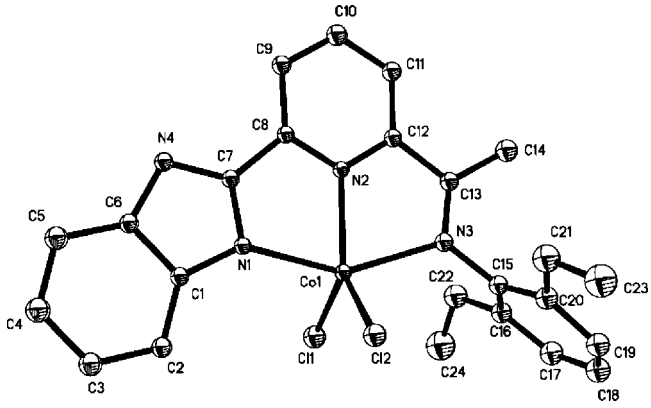

Figure 2. ORTEP drawing of complex **Co2** with thermal ellipsoids at 30% probability. Hydrogen atoms have been omitted for clarity.

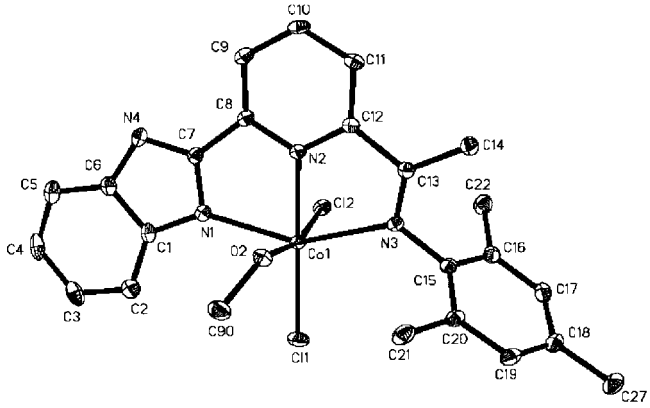

Figure 3. ORTEP drawing of complex **Co4** with thermal ellipsoids at 30% probability. Hydrogen atoms have been omitted for clarity.

Table 2. Selected Bond Lengths (Å) and Angles (deg) for Co4

Co(1)−N(1)	2.171(3)	Co(1)−N(2)	2.094(3)
Co(1)−N(3)	2.216(3)	Co(1)−Cl(1)	2.282(1)
Co(1)−Cl(2)	2.553(1)	N(1)−C(7)	1.323(5)
N(4)−C(7)	1.350(4)	N(3)−C(13)	1.279(4)
Co(1)−O(2)	2.260(3)	N(3)−Co(1)−O(2)	89.15(10)
N(1)−Co(1)−N(2)	75.53(11)	N(1)−Co(1)−N(3)	149.16(11)
N(2)−Co(1)−N(3)	73.88(11)	N(1)−Co(1)−Cl(1)	105.33(8)
N(2)−Co(1)−Cl(1)	176.90(8)	N(3)−Co(1)−Cl(1)	105.01(8)
Cl(1)−Co(1)−Cl(2)	95.29(4)	N(1)−Co(1)−Cl(2)	89.16(8)
N(2)−Co(1)−Cl(2)	87.69(8)	N(3)−Co(1)−Cl(2)	93.42(8)
N(2)−Co(1)−O(2)	81.75(10)	N(1)−Co(1)−O(2)	82.69(10)

(Figure 3) in which the cobalt atom is surrounded by one ligand, two chloride atoms, and one methanol molecule. Selected bond lengths and angles are listed in Table 2. The Co(1) atom deviates by 0.0333 Å out of the N(1)−N(2)−N(3) plane, while the chlorine atom Cl(1) is almost coplanar with a deviation of 0.0156 Å from the equatorial plane of three nitrogen atoms. The other chlorine atom, Cl(2), and the O atom of coordinated methanol (O(2)) occupy the axial position and form an angle of 167.99(7)° with the cobalt core. The axial plane is nearly perpendicular to the equatorial plane with a dihedral angle of 90.4°. The 2,4,6-trimethylphenyl ring and the equatorial plane form a dihedral angles of 112.6°. It is not common for cobalt complexes to form a distorted octahedral coordination geometry with one additional solvent molecule, but one example was obtained in our previous work,[26] while there were several cases for iron complexes.[20]

Table 3. Selection of Suitable Cocatalyst[a]

entry	cocatalyst	Al/Fe	oligomer distribn[b]	oligomer activity[c]	polymer activity[d]
1	MAO	1000	C_4-C_{28}	26.2	2.9
2	MMAO	1000	C_4-C_{30}	41.1	3.4
3	Et_2AlCl	200	C_4, C_6	0.7	

[a] Reaction conditions: 5 μmol of complex **Fe3**; 10 atm of ethylene; 20 °C; 30 min; 100 mL of toluene. [b] Oligomer distribution determined by GC. [c] Oligomer activity (10^5 g·mol^{-1}(Fe)·h^{-1}). [d] Polyethylene wax activity (10^5 g·mol^{-1}(Fe)·h^{-1}).

2.3. Catalytic Behavior of Metal Complexes in Ethylene Reactivity. As the target in the current study, the catalytic behavior of metal complexes ligated by 2-(1*H*-benzimidazolyl)-6-(1-aryliminoethyl)pyridines is evaluated in order to find suitable cocatalysts and optimum conditions for the catalytic reactions. The two groups of iron and cobalt complexes are investigated separately.

2.3.1. Catalytic Behavior of Fe(II) Complexes. The catalytic activities of Fe(II) complex **Fe3** were determined in the presence of different cocatalysts such as MAO, MMAO, and Et_2AlCl. Due to low catalytic activity and mostly ethylene dimerization at ambient pressure of ethylene, the elevated pressure of 10 atm ethylene was employed for selecting suitable cocatalysts. As shown in Table 3, both **Fe3**/MAO and **Fe3**/MMAO systems exhibited good activity toward ethylene oligomerization along with considerable activity for ethylene polymerization; however, the **Fe3**/Et_2AlCl system showed lower activity for dimerization and trimerization of ethylene. Therefore, the catalytic systems with MAO and MMAO were separately investigated in detail.

2.3.1.1. Ethylene Reactivity in the Presence of MAO. In the presence of MAO as cocatalyst, all iron complexes were investigated for their ethylene reactivity, and the results are summarized in Table 4. The complex **Fe3** was investigated in detail for the optimum reaction conditions through varying ethylene pressure, Al/Fe molar ratio, and reaction temperature.

The catalytic performance of **Fe3** was tested under different ethylene pressures. Considerable activity was observed for its ethylene dimerization along with additional oligomers in the range C6−C10 at ambient ethylene pressure (entry 1 of Table 4), while high activity of full-range ethylene oligomerization was obtained at 10 atm of ethylene pressure (entry 3, Table 4). Moreover, better selectivity for α-olefins was observed at elevated ethylene pressure. The higher the ethylene pressure used, the faster the ethylene coordination on the active species and the higher the activity observed. An acceptable plausible mechanism for better selectivity of α-olefins at elevated ethylene pressure was well explained in a review article.[3] At low ethylene pressure, there was less ethylene coordinated on the active species and the intermediate species would undergo β-hydrogen elimination before ethylene coordination and further chain migration, producing inert and branched oligomers (path A, Scheme 5). At higher ethylene pressure, ethylene coordination occurred before β-hydride elimination of the chain; however, direct β-hydride transfer of the chain to coordinated ethylene occurred to give an α-olefin during competition of further propagation and chain transfer (path B, Scheme 5). Considering the oligomer distribution and the selectivity for α-olefins, it would be interesting to carry out further investigations at 10 atm of ethylene pressure.

Two possible paths resulted in different selectivity of α-olefins: (A) partial chain migration due to less ethylene around the active site; (B) oligomer produced with direct β-hydride transfer to coordinated ethylene.

Table 4. Polymerization and Oligomerization of Ethylene with Fe1−Fe6/MAO[a]

				oligomers[b]							
entry	cat.	Al/Fe	*T*/°C	$C_4/\Sigma C$	$C_6/\Sigma C$	$C_8/\Sigma C$	$\geq C_{10}/\Sigma C$	*K*	α-O (%)	A_o[c]	polymer[d]
1[e]	**Fe3**	1000	20	69.8	18.7	7.4	4.1		≥70	0.9	
2	**Fe3**	500	20	61.2	19.4	11.1	8.3		≥99	5.8	trace
3	**Fe3**	1000	20	40.6	26.5	13.1	19.8	0.53	≥99	26.2	2.9
4	**Fe3**	1500	20	38.2	23.7	15.4	22.7	0.58	≥98	11.6	1.8
5	**Fe3**	1000	40	61.9	16.8	8.5	12.8	0.52	≥87	6.2	0.2
6	**Fe3**	1000	60	69.5	17.6	6.7	6.2	0.55	≥75	1.4	trace
7	**Fe1**	1000	20	35.5	17.8	12.2	34.5	0.42	≥99	13.5	8.2
8	**Fe2**	1000	20	42.1	15.2	11.7	32.0	0.51	≥99	15.7	2.1
9	**Fe4**	1000	20	37.8	15.4	12.7	34.1	0.46	≥99	3.9	3.5
10	**Fe5**	1000	20	45.3	19.5	8.7	26.5	0.43	≥97	1.6	0.3
11	**Fe6**	1000	20	47.8	20.7	11.2	20.3	0.62	≥97	2.7	0.5

[a] Reaction conditions: 5 μmol of Fe(II) complex; 10 atm of ethylene; 30 min; 100 mL of toluene. [b] Oligomer distributions and α-olefin content determined by GC. [c] Activity of oligomerization: 10^5 g·mol^{-1}(Fe)·h^{-1}. [d] Activity of polyethylene wax: 10^5 g·mol^{-1}(Fe)·h^{-1}. [e] 1 atm of ethylene; 30 min; 30 mL of toluene.

Scheme 5. Two Plausible Termination Mechanisms

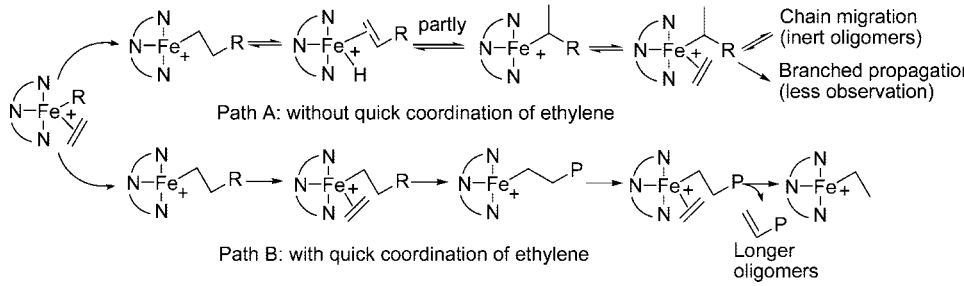

The amount of cocatalyst MAO significantly affected the catalytic results. At 10 atm of ethylene pressure and Al/Fe molar ratios of 500, 1000, and 1500 (entries 2−4, Table 4), the best performance was obtained at the ratio of 1000. There were no more short-chain oligomers with an increase in the Al/Fe molar ratios. In addition, polyethylene waxes were obtained at ratios of 1000 and 1500. The distribution of oligomers obtained approximately resembles Schulz−Flory rules, which is characterized by the constant *K* [*K* = rate of propagation/(rate of propagation + rate of chain transfer) = moles of C_{n+2}/moles of C_n].[39−43] The *K* values are determined by the molar ratio of C_{12} and C_{14} fractions. Increasing the Al/Fe ratio from 500 to 1500 results in sharply increasing *K* values (entries 2−4, Table 4), and longer chain oligomers were formed. These results do not support chain transfer from Fe active site to Al active site at higher Al/Fe ratio; at least, the chain transfer from the Fe active site to the Al active site at higher Al/Fe ratio did not affect the final catalytic activity. In other words, these results support that the most active species is created at the Al/Fe ratio of 1000.

The influence of reaction temperature on the catalytic activity was further investigated in the catalytic system of **Fe3** at the Al/Fe molar ratio of 1000 at 10 atm of ethylene pressure. When reaction temperature changed from 20 to 60 °C, the catalytic activity was decreased and lesser amounts of longer chain oligomers were observed. This could be caused by the lower solubility of ethylene and lesser stability of active species at higher temperature.[9] Therefore, the optimum condition was used in measuring catalytic activities of all iron complexes with the Al/Fe molar ratio of 1000 at 10 atm of ethylene pressure and 20 °C.

With the optimized conditions, the catalytic behaviors toward ethylene reactivity by iron complexes **Fe1**−**Fe6** are listed in Table 4. There are significant influences of ligands on the catalytic activities of their iron complexes (entries 3 and 7−11, Table 4), in which the steric effects of ligands likely played major roles, especially the substituents in *ortho*-position of the aryl group in the aryliminoethyl part. Comparing the data from entries 3, 7, and 8 in Table 4, it was clear that the highest catalytic activity (for ethylene oligomerization and combined activity) was obtained by **Fe3**, which contains a 2,6-diisopropylphenyl group. Their oligomerization activities varied, with higher activity observed with bulky substituents on the *ortho*-position of the aryl group in the aryliminoethyl part: the activity of **Fe3** (with 2,6-diisopropyl substituents, 2.62×10^6 g·mol^{-1}(Fe)·h^{-1}, entry 3 of Table 4) is higher than that of **Fe2** (with 2,6-diethyl substituents, 1.57×10^6 g·mol^{-1}(Fe)·h^{-1}, entry 8 of Table 4), and both are higher than that of **Fe1** (with 2,6-dimethyl substituents, 1.35×10^6 g·mol^{-1}(Fe)·h^{-1}, entry 7 of Table 4). Moreover, the three corresponding *K* values follow the same trend (entries 3, 7, and 8), which indicates that higher *K* values were favored with increasing steric demand. The same trend was also observed in the catalytic systems of their analogues ligated by 2-(1-methyl-2-benzimidazolyl)-6-(1-(arylimino)ethyl)pyridines[23] and 2-(1-isopropyl-2-benzimidazolyl)-6-(1-(arylimino)ethyl)pyridines.[24] For the catalytic performance by complexes **Fe5** and **Fe6**, the same steric influence was reflected because **Fe6**, with dibromo substituents, gave better activity than **Fe5**, with dichloro substituents. The bulkier the substituents at the *ortho*-position of the aryl group, the lesser amounts of longer chain oligomers observed. It might be explained that bulkier substituents slow ethylene coordination and hinder chain propagation. These results were consistent with results obtained with their analogues.[23,24] However, it is

(39) Flory, P. J. *J. Am. Chem. Soc.* **1940**, *62*, 1561.
(40) Schulz, G. V. Z. *Phys. Chem., Abt. B* **1935**, *30*, 379.
(41) Schulz, G. V. Z. *Phys. Chem., Abt. B* **1939**, *43*, 25.
(42) Meurs, M. V.; Britovsek, G. J. P.; Gibson, V. C.; Cohen, S. A. *J. Am. Chem. Soc.* **2005**, *127*, 9913.
(43) Britovsek, G. J. P.; Cohen, S. A.; Gibson, V. C.; Meurs, M. V. *J. Am. Chem. Soc.* **2004**, *126*, 10701.

Table 5. Ethylene Reactivity by Fe1−Fe6/MMAO[a]

					oligomers[b]							
entry	cat.	Al/Fe	*t*/min	*T*/°C	$C_4/\Sigma C$	$C_6/\Sigma C$	$C_8/\Sigma C$	$\geq C_{10}/\Sigma C$	*K*	α-O(%)	A_o[c]	polymer[d]
1[e]	**Fe3**	1000	30	20	69.7	20.2	7.5	3.6		≥73	1.2	trace
2	**Fe3**	500	30	20	65.7	16.4	14.0	3.9	0.60	≥99	3.7	trace
3	**Fe3**	800	30	20	51.3	21.1	12.3	10.6	0.62	≥99	19.8	0.9
4	**Fe3**	1000	30	20	42.5	24.6	14.7	18.2	0.46	≥99	41.1	3.4
5	**Fe3**	1200	30	20	34.6	25.5	14.1	25.8	0.57	≥98	33.5	1.4
6	**Fe3**	1500	30	20	39.1	24.9	14.5	21.5	0.52	≥97	29.0	1.3
7	**Fe3**	1000	30	40	63.4	13.8	10.8	12.0	0.43	≥90	4.5	0.7
8	**Fe3**	1000	30	60	67.5	16.4	8.2	7.9	0.59	≥81	1.3	0.2
9	**Fe3**	1000	60	20	40.7	23.1	13.7	22.5	0.51	≥98	23.4	2.1
10	**Fe1**	1000	30	20	30.5	19.2	18.8	32.5	0.50	≥99	17.2	7.4
11	**Fe2**	1000	30	20	31.5	19.6	15.6	26.5	0.55	≥99	12.9	2.0
12	**Fe4**	1000	30	20	27.1	21.9	18.4	32.6	0.47	≥99	5.2	5.6
13	**Fe5**	1000	30	20	41.7	19.1	7.9	31.3	0.61	≥98	4.6	0.6
14	**Fe6**	1000	30	20	51.2	19.6	12.1	17.1	0.55	≥95	2.4	0.2

[a] Reaction conditions: 5 μmol of Fe(II) complex; 10 atm of ethylene; 100 mL of toluene. [b] Determined by GC. [c] In units of 10^5 g·mol^{-1}(Fe)·h^{-1}. [d] Activity for polyethylene wax: 10^5 g·mol^{-1}(Fe)·h^{-1}. [e] 1 atm of ethylene; 30 min; 30 mL of toluene.

Table 6. Ethylene Oligomerization by Co1−Co6/MMAO[a]

							oligomers[c]		
entry	cat.	cocat.	Al/Co	*P*/atm	*T*/°C	A_o[b]	$C_4/\Sigma C$	$C_6/\Sigma C$	α-C_4%
1[d]	**Co1**	MAO	1000	1	20	0.7	100		≥95
2[d]	**Co1**	MMAO	1000	1	20	1.1	100		≥89
3	**Co1**	MAO	1000	10	20	8.6	96.4	3.6	≥94
4	**Co1**	Et_2AlCl	200	10	20	5.8	98.5	1.5	≥96
5	**Co1**	MMAO	1000	10	20	15.1	95.5	4.5	≥92
6	**Co1**	MMAO	500	10	20	1.5	80.4	19.6	≥95
7	**Co1**	MMAO	1500	10	20	8.1	89.6	10.4	≥97
8	**Co1**	MMAO	1000	10	40	5.5	85.6	4.4	≥86
9	**Co1**	MMAO	1000	10	60	3.7	78.5	11.5	≥78
10	**Co2**	MMAO	1000	10	20	10.3	94.6	5.4	≥91
11	**Co3**	MMAO	1000	10	20	8.7	95.3	4.7	≥95
12	**Co4**	MMAO	1000	10	20	7.1	94.3	5.7	≥90
13	**Co5**	MMAO	1000	10	20	5.0	92.7	7.3	≥95
14	**Co6**	MMAO	1000	10	20	3.6	94.1	5.9	≥97

[a] Reaction conditions: 5 μmol of Co(II) complex; 10 atm of ethylene; 30 min; 100 mL of toluene. [b] In units of 10^4 g·mol^{-1}(Co)·h^{-1}. [c] Determined by GC. [d] 1 atm of ethylene; 30 mL of toluene.

surprising that the iron complex **Fe4**, bearing a 2,4,6-trimethylphenyl group, showed very low activity. Even though some amounts of polyethylene waxes were obtained in some cases, the oligomers were major products. Moreover, the high selectivity for the α-olefins is also the important advantage of considering the iron catalytic system for a full range of ethylene oligomerization.

In comparison with their analogues with alkylated benzimidazoles, the catalytic system of the title iron complex with a remaining N−H group on the benzimidazole showed higher activity. The complexes containing 2,6-dimethylphenyl substituents in the aryliminoethyl parts are compared as an typical example; ethylene oligomerization activities of 1.35×10^6 g·mol^{-1}(Fe)·h^{-1} are observed in this research (**Fe1**, entry 7 in Table 4) with a remaining N−H group and 9.2×10^5 g·mol^{-1}(Fe)·h^{-1} for its analogue with an N−Me group[23] (for **7a**, entry 3 of Table 6 in ref 23) and 2.34×10^5 g·mol^{-1}(Fe)·h^{-1} for its analogue with an N−^{i}Pr group[24] (for **1a**, entry 3 of Table 5 in ref 24). The better catalytic activities for complexes containing ligands with a remaining N−H group on the benzimidazole are potentially caused by the formation of anionic amides or N−Al species in situ when the organoaluminum cocatalyst is added. The active species of ion pair states are commonly proposed in metallocene catalysts[44,45] and also approved in late transition metal catalysts.[46] The image of active species is not clear yet in this work, and further research is under way.

2.3.1.2. Ethylene Reactivity in the Presence of MMAO. Similarly to the **Fe3**/MAO catalyst system, we employed a routine procedure to investigate the **Fe3**/MMAO system and found the same phenomena: the productivity dramatically increased when increasing ethylene pressure from 1 atm (entry 1, Table 5) to 10 atm (entry 4, Table 5), and a higher selectivity for α-olefins was observed at elevated ethylene pressure. The Al/Fe molar ratios were varied at 10 atm (entries 2−6, Table 5). The **Fe3**/MMAO system had the best activity at the Al/Fe molar ratios of 1000. The system required an excessive amount of cocatalyst MMAO for scavenging impurities from solvents or gas and producing active species; however, a greater excess of MMAO higher than the Al/Fe ratio 1000:1 resulted in a lower activity due to hindering the insertion reaction of ethylene by the isobutyl group,[47,48] and the most active species was formed at an Al/Fe ratio of 1000:1.

An increase in reaction temperature resulted in a lower catalytic activity as well as a lower amount of longer chain oligomers (entries 4, 7, and 8, Table 5), which is consistent with a lower absorption of ethylene in solution and a decrease in stability of the active species at higher temperature. In addition, the selectivity for α-olefins decreases along with elevating the reaction temperature. Ethylene consumption was smoothly maintained for about half an hour, and deactivation of the active species was observed at extended reaction times (entries 4 and 9, Table 5).

The influence of substituents on the catalytic activities of the iron complexes and their oligomer distributions with MMAO follow the same trends observed in the Fe(II)/MAO systems. Complexes **Fe1**, **Fe2**, **Fe3**, and **Fe4**, with an alkylphenyl group (entries 4, 10−12, Table 5), showed higher activity than complexes **Fe5** and **Fe6**, with a halogen group (entries 13, 14, Table 5). The steric effect of ligands played an important role (entries 4, 10−12, Table 5), with less bulky substituents

(44) Bochmann, M. *J. Organomet. Chem.* **2004**, *689*, 3982.
(45) Alonso-Moreno, C.; Lancaster, S. J.; Wright, J. A.; Hughes, D. L.; Zuccaccia, C.; Correa, A.; Macchioni, A.; Cavallo, L.; Bochmann, M. *Organometallics* **2008**, *27*, 5474.
(46) Anselment, T. M. J.; Vagin, S. I.; Rieger, B. *Dalton Trans.* **2008**, 4537.
(47) Chen, E. Y. X.; Marks, T. J. *Chem. Rev.* **2000**, *100*, 1391.
(48) Karam, A. R.; Catarí, E. L.; López-Linares, F.; Agrifoglio, G.; Albano, C. L.; Díaz-Barrios, A.; Lehmann, T. E.; Pekerar, S. V.; Albornoz, L. A.; Atencio, R.; González, T.; Ortega, H. B.; Joskowics, P. *Appl. Catal. A: Gen.* **2005**, *280*, 165.

rendering the active sites of the catalyst exposed to both ethylene and other active species, which deactivated the active species.[9] Basically all catalytic systems approximately resemble Schulz−Flory rules; however, an exception is the catalytic system **Fe5**, containing electron-withdrawing chloride, which deviates from Schulz−Flory rules.

The iron complex with a remaining N−H group on the benzimidazole showed higher activity than its analogues with alkylated benzimidazoles with the assistance of MMAO. The 2-(2-benzimidazolyl)-6-(1-aryliminoethyl)pyridyliron dichloride, **Fe1**, had an ethylene oligomerization activity of 1.72×10^6 $g \cdot mol^{-1}(Fe) \cdot h^{-1}$ (entry 10, Table 5), while the 2-(1-methyl-2-benzimidazolyl)-6-(1-aryliminoethyl)pyridyliron dichloride showed an activity of 1.2×10^6 $g \cdot mol^{-1}(Fe) \cdot h^{-1}$ (entry 5 of Table 7 in ref 23).[23]

2.3.2. Ethylene Oligomerization of Co(II) Complexes. In comparison with their iron analogues, cobalt complexes showed much lower catalytic activities toward ethylene. This is apparent for metal complexes ligated by bis(imino)pyridines[9] and various systems.[23,25,49] The low activity was observed at ambient pressure of ethylene (entries 1 and 2, Table 6); therefore the selections of suitable cocatalysts and Al/Co molar ratios were carried out with the complex **Co1** at 10 atm ethylene (entries 3−5, Table 6), with the most suitable one being MMAO. The catalytic system performed with highest activity at the MMAO/Co1 molar ratio of 1000 (entries 5−7, Table 6). The catalytic behaviors by cocatalysts in cobalt complexes containing an N−H group on the benzimidazole are different from their analogues with alkylated benzimidazoles. Moreover, better catalytic performance was observed at lower reaction temperature (entries 5, 8, 9, Table 6). Using optimum reaction conditions, all cobalt complexes were tested for ethylene oligomerization (Table 6).

Similarly to their iron analogues, the cobalt complexes **Co1**, **Co2**, **Co3**, and **Co4**, with alkylphenyl groups (entries 5, 10−12, Table 6), showed higher activity than complexes **Co5** and **Co6**, with halogen groups (entries 13, 14, Table 6). However, different steric influence was observed in the catalytic system of Co(II) complexes: the less bulky substituents the cobalt complexes contained, the higher the catalytic activity (entries 5, 10−11, Table 6).

3. Conclusion

The methodology for synthesizing 6-(1*H*-2-benzimidazolyl)-2-acetylpyridine was well developed; therefore the title metal complexes were prepared. All title complexes produced oligomers with high selectivity for α-olefins, and an increase in selectivity for α-olefins was observed at elevated ethylene pressure. Elevated reaction temperature reduced the catalytic activity. The cobalt complexes performed with considerable to moderate catalytic activity toward ethylene oligomerization with the assistance of MMAO. In the presence of either MAO or MMAO as cocatalyst, all iron complexes performed with high catalytic activities toward ethylene oligomerization along with considerable activity for ethylene polymerization. The iron complexes with an alkylphenyl group showed higher activity than the complexes with a halogenated phenyl group, and higher activity was obtained with bulky substituents on the *ortho*-position of the aryl group in the aryliminoethyl part. In a typical example, the iron complex with a remaining N−H group on the benzimidazole showed higher activity than its analogues with alkylated benzimidazoles.[23,24]

4. Experimental Section

4.1. General Considerations. All manipulations of air- and moisture-sensitive compounds were performed under a nitrogen atmosphere using standard Schlenk techniques. Methylaluminoxane and modified methylaluminoxane were purchased from AkzoNobel Corp. Diethylaluminum chloride was purchased from Acros Chemicals; ^1H and ^{13}C NMR spectra were recorded on a Bruker DMX 300 MHz instrument at ambient temperature using TMS as an internal standard. FT-IR spectra were recorded on a Perkin-Elmer System 2000 FT-IR spectrometer. Elemental analysis was carried out using an HPMOD 1106 microanalyzer. GC analysis was performed with a Carlo Erba Strumentazione gas chromatograph equipped with a flame ionization detector and a 30 m (0.2 mm i.d., 0.25 μm film thickness) DM-1 silica capillary column. The yield of oligomers was calculated by referencing to the mass of the solvent on the basis of the prerequisite that the mass of each fraction was approximately proportional to its integrated area in the GC trace. Ethylene oligomerization and polymerization were performed in a stainless steel autoclave (0.5 L capacity) equipped with a gas ballast through a solenoid clave for continuous feeding of ethylene at constant pressure.

4.2. Synthesis of 2-(1*H*-Benzimidazolyl)-6-acetylpyridine. A solution of *o*-phenylenediamine (2.16 g, 0.020 mol), diethyl 2,6-bis(β-keto-carboxylate)pyridine (6.15 g, 0.020mol), and a catalytic amount of *p*-toluenesulfonic acid in toluene and isopropyl alcohol (60 mL, v/v = 3:1) was refluxed for 12 h. Most of the solvent was evaporated, and a mixture of 20 mL of acetic acid and 5 mL of concentrated HCl was added. Then the mixture was refluxed for 6 h. After the mixture was cooled to room temperature, a 20% KOH solution was added, until the pH was close to 9−10. The aqueous phase was shaken with CH_2Cl_2 (15 mL × 3). The combined extracts were dried over anhydrous Na_2SO_4 and filtered, and the solvent was finally evaporated at reduced pressure. The desired compound 2-acetyl-6-(1*H*-2-benzimidazolyl)pyridine was obtained as 1.05 g of a white solid (21% isolated yield) after purification by column chromatography (silica gel, petroleum ether/ethyl acetate/acetone = 6:2:1 (v/v)). Mp: 186−187 °C. ^1H NMR (300 MHz, $CDCl_3$, TMS): δ 10.39 (brs, 1H, NH), 8.62 (d, 1H, J = 7.7 Hz, Py), 8.12 (d, 1H, J = 7.7 Hz, Py), 8.02 (t, 1H, J = 7.8 Hz, Py), 7.87 (d, 1H, J = 7.2 Hz, Ar), 7.59 (d, 1H, J = 6.8 Hz, Ar), 7.36 (m, 2H, Ar), 2.86 (s, 3H, CH_3). ^{13}C NMR (75 MHz, $CDCl_3$, TMS): δ 199.4, 153.1, 150.1, 147.9, 144.4, 138.4, 134.1, 125.0, 124.5, 123.1, 122.5, 120.3, 111.6, 25.9. IR (KBr; cm^{-1}): 3387 (w), 3051 (m), 2929 (w), 1705 (vs), 1592 (s), 1459 (s), 1421(s), 1388 (m), 1357 (m), 1314 (m), 1278 (w), 1224 (m), 1151 (m), 1123 (m), 994 (w), 823 (m), 745 (s). Anal. Calcd for $C_{14}H_{11}N_3O$ (237.26): C, 70.87; H, 4.67; N, 17.71. Found: C, 71.06; H, 4.70; N, 17.67.

A mixture of *o*-phenylenediamine (1.08 g, 0.01 mol), diethyl 2,6-bis(β-keto-carboxylate)pyridine (3.08 g, 0.010 mol), and a catalytic amount of *p*-toluenesulfonic acid dissolved in 30 mL of toluene and 10 mL of propanol was refluxed for 10 h. After evaporating the solvent at reduced pressure and purification of the residual solids by column chromatography (silica gel, petroleum ether/ethyl acetate (5:1, v/v)), 0.90 g (29% isolated yield) of the desired compound, ethyl 6-(1*H*-benzmidazol-2-yl)pyridine-2-carboxylate, was isolated as a white solid. Mp: 182−183 °C. ^1H NMR (300 MHz, $CDCl_3$): δ 10.61 (brs, 1H, NH), 8.60 (dd, J_1 = 0.8 Hz, J_2 = 7.6 Hz, 1H, Py), 8.05 (m, 2H, Py), 7.87 (d, J = 7.8 Hz, 1H, Ar), 7.65 (d, J = 7.6 Hz, 1H, Ar), 7.36 (m, 2H, Ar), 4.15 (q, 2H, J = 7.2 Hz, CH_2), 4.05 (s, 2H, CH_2), 1.08 (t, 3H, J = 7.2 Hz, CH_3). ^{13}C NMR (75 MHz, $CDCl_3$): δ 192.67, 169.23, 151.10, 149.68, 147.68, 138.80, 125.02, 122.30, 61.63, 47.59, 13.90. FT-IR (KBr; cm^{-1}): 3400 (w), 3047 (m), 2981 (w), 1735 (m), 1709

(49) Bianchini, C.; Mantovani, G.; Meli, A.; Migliacci, F.; Zanobini, F.; Laschi, F.; Sommazzi, A. *Eur. J. Inorg. Chem.* **2003**, 1620.

(s), 1593 (s), 1460 (s), 1421 (s), 1388 (m), 1316 (m), 1278 (m), 1153 (m), 1006 (w), 992 (m), 825 (w), 747 (m), 671 (s). Anal. Calcd for $C_{17}H_{15}N_3O_2$ (309.32): C, 66.01; H, 4.89; N, 13.58. Found: C, 65.94; H, 4.85; N, 13.64.

4.3. Synthesis of Tridentate Ligands L1−L6: (*E*)-2,6-Dimethyl-*N*-(1-(6-(1*H*-benzo[*d*]imidazol-2-yl)pyridin-2-yl)ethylidene)benzenamine (L1). A mixture of 2-acetyl-6-(1*H*-2-benzimidazolyl)pyridine (474 mg, 2 mmol), 2,6-dimethylaniline (302 mg, 2.5 mmol), and a catalytic amount of *p*-toluenesulfonic acid dissolved in toluene (25 mL) was refluxed for 24 h. After solvent evaporation, the crude product was purified by column chromatography on basic Al_2O_3 with petroleum ether/ethyl acetate (v/v = 3:1) as eluent to afford the product as a light yellow powder in 68.3% yield. Mp: 194−195 °C. ^{1}H NMR (300 MHz, CDCl $_3$, TMS): δ 10.42 (brs, 1H, NH), 8.54 (d, 1H, J = 7.8 Hz, Py), 8.52 (t, 1H, J = 7.6 Hz, Py), 8.44(t, 1H, J = 7.8, Py), 7.99 (d, 1H, J = 7.8 Hz, Ar), 7.56 (d, 1H, J = 7.6 Hz, Ar), 7.35 (m, 2H, Ar), 7.11 (d, 2H, J = 7.5 Hz, Ar), 6.98 (t, 1H, J = 7.4 Hz, Ar), 2.31 (s, 3H, CH_3), 2.06 (s, 6H, CH_3). ^{13}C NMR (75 MHz, $CDCl_3$, TMS): δ 166.5, 156.1, 150.8, 148.7, 147.3, 144.6, 137.9, 133.8, 128.1, 125.5, 124.2, 123.4, 123.0, 122.8, 122.3, 120.3, 111.4, 18.1, 16.8. IR (KBr; cm^{-1}): 3447 (w), 3066 (m), 2953 (m), 2922 (m), 1648 (vs), 1592 (s), 1569 (s), 1464 (vs), 1420 (vs), 1385 (w), 1318 (s), 1278 (w), 1206 (s), 1125 (m), 1092 (w), 993 (w), 823 (w), 767 (m), 744 (vs). Anal. Calcd for $C_{22}H_{20}N_4$ (340.42): C, 77.62; H, 5.92; N, 16.46. Found: C, 77.59; H, 5.95; N, 16.42.

(*E*)-2,6-Diethyl-*N*-(1-(6-(1*H*-benzo[*d*]imidazol-2-yl)pyridin-2-yl)ethylidene)benzenamine (L2). Using the same procedure as for the synthesis of **L1**, **L2** was obtained as a light yellow powder in 61.5% yield. Mp: 235−236 °C. ^{1}H NMR (300 MHz, $CDCl_3$, TMS): δ 10.46 (brs, 1H, NH), 8.54 (d, 1H, J = 7.8 Hz, Py), 8.45 (d, 1H, J = 8.1 Hz, Py), 8.00 (t, 1H, J = 7.8 Hz, Py), 7.89 (m, 1H, Ar), 7.57 (d, 1H, J = 6.0 Hz, Ar), 7.27 (m, 2H, Ar), 7.14 (d, 2H, J = 8.1 Hz, Ar), 7.08 (m, 1H, Ar), 2.56 (q, 4H, J = 7.5 Hz, CH_2), 2.31 (s, 3H, CH_3), 1.15 (t, 6H, J = 7.5 Hz, CH_3). ^{13}C NMR (75 MHz, $CDCl_3$, TMS): δ 166.3, 156.0, 150.8, 147.7, 147.3, 144.6, 138.0, 133.9, 131.2, 126.1, 124.2, 123.6, 122.7, 122.3, 120.3, 111.5, 24.7, 17.1, 13.9. IR (KBr; cm^{-1}): 3449 (w), 3060 (w), 2964 (s), 2931 (m), 2872 (w), 1650 (vs), 1591 (vs), 1569 (vs), 1462 (vs), 1421 (vs), 1386 (w), 1364 (m), 1318 (s), 1279 (m), 1239 (w), 1226 (w), 1197 (m), 1127 (m), 1010 (w), 993 (m), 823 (m), 781 (m), 745 (vs). Anal. Calcd for $C_{24}H_{24}N_4$ (368.47): C, 78.23; H, 6.57; N, 15.21. Found: C, 78.25; H, 6.59; N, 15.15.

(*E*)-2,6-Diisopropyl-*N*-(1-(6-(1*H*-benzo[*d*]imidazol-2-yl)pyridin-2-yl)ethylidene)benzenamine (L3). Using the same procedure as for the synthesis of **L1**, **L3** was obtained as a light yellow powder in 77.3% yield. Mp: 256−257 °C. ^{1}H NMR (300 MHz, $CDCl_3$, TMS): δ 10.44 (brs, 1H, NH), 8.53 (d, 1H, J = 7.8 Hz, Py), 8.45 (d, 1H, J = 7.5 Hz, Py), 8.01 (t, 1H, J = 7.8 Hz, Py), 7.88 (d, 1H, J = 6.1 Hz, Ar), 7.56 (d, 1H, J = 6.1 Hz, Ar), 7.33 (m, 2H, Ar), 7.19 (m, 2H, Ar), 7.12 (m, 1H, Ar), 2.78 (m, 2H, CH), 2.33 (s, 3H, CH_3), 1.18 (d, 12H, J = 6.6 Hz, CH_3). ^{13}C NMR (75 MHz, $CDCl_3$, TMS): δ 166.3, 156.0, 150.8, 147.3, 146.4, 144.6, 138.0, 135.9, 133.9, 132.6, 124.2, 123.9, 123.2, 123.0, 122.7, 122.4, 120.3, 111.5, 28.5, 23.4, 23.0, 22.6, 17.5. IR (KBr; cm^{-1}): 3460 (w), 3046 (w), 2962 (vs), 1655 (vs), 1592 (s), 1569 (vs), 1463 (vs), 1421 (vs), 1386 (s), 1340 (s), 1317 (s), 1278 (w), 1227 (m), 1191 (w), 1128 (w), 1110 (m), 992 (m), 935 (w), 824 (m), 778 (s), 745 (vs). Anal. Calcd for $C_{26}H_{28}N_4$ (396.53): C, 78.75; H, 7.12; N, 14.13. Found: C, 78.69; H, 7.15; N, 14.09.

(*E*)-2,4,6-Trimethyl-*N*-(1-(6-(1*H*-benzo[*d*]imidazol-2-yl)pyridin-2-yl)ethylidene)benzenamine (L4). Using the same procedure as for the synthesis of **L1**, **L4** was obtained as a light yellow powder in 58.2% yield. Mp: 211−212 °C. ^{1}H NMR (300 MHz, $CDCl_3$, TMS): δ 10.45 (brs, 1H, NH), 8.53 (d, 1H, J = 7.7 Hz, Py), 8.43 (d, 1H, J = 7.2 Hz, Py), 8.00 (t, 1H, J = 7.8 Hz, Py), 7.89 (t, 1H, J = 5.0 Hz, Ar), 7.58 (t, 1H, J = 3.7 Hz, Ar), 7.33 (m, 2H, Ar), 6.92 (s, 2H, Ar), 2.31 (s, 3H, CH_3), 2.30 (s, 3H, CH_3), 2.03 (s, 6H, CH_3). ^{13}C NMR (75 MHz, $CDCl_3$, TMS): δ 166.5, 155.9, 150.6, 147.1, 145.9, 144.4, 137.7, 133.7, 132.4, 128.5, 125.1, 124.0, 122.8, 122.5, 122.1, 120.1, 111.2, 20.7, 17.9, 16.5. IR (KBr; cm^{-1}): 3446 (w), 3000 (w), 2962 (w), 2913 (m), 1647 (vs), 1592 (s), 1570 (vs), 1490 (w), 1460 (s), 1420 (m), 1385 (m), 1362 (m), 1308 (m), 1279 (m), 1215 (s), 1147 (m), 1121 (s), 1011 (m), 992 (w), 856 (s), 824 (m), 789 (w), 767 (w), 745 (vs). Anal. Calcd for $C_{23}H_{22}N_4$ (354.45): C, 77.94; H, 6.26; N, 15.81. Found: C, 77.95; H, 6.31; N, 15.72.

(*E*)-2,6-Dichloro-*N*-(1-(6-(1*H*-benzo[*d*]imidazol-2-yl)pyridin-2-yl)ethylidene)benzenamine (L5). Using a similar procedure to that for the synthesis of **L1**, with silicic acid tetraethyl ester employed as solvent instead of toluene, **L5** was obtained as a white powder in 31.6% yield. Mp: 160−162 °C. ^{1}H NMR (300 MHz, $CDCl_3$, TMS): δ 10.39 (brs, 1H, NH), 8.56 (d, 1H, J = 7.6 Hz, Py), 8.45 (d, 1H, J = 7.8 Hz, Py), 8.02(t, 1H, J = 7.8 Hz, Py), 7.88 (s, 1H, Ar), 7.58 (s, 1H, Ar), 7.38 (m, 4H, Ar), 7.03 (t, 1H, J = 8.0 Hz, Ar), 2.43(s, 3H, CH_3). ^{13}C NMR (75 MHz, $CDCl_3$, TMS): δ 170.7, 155.2, 150.5, 147.4, 145.5, 144.6, 138.1, 133.8, 128.4, 124.7, 124.6, 124.3, 123.3, 123.1, 120.4, 111.4, 17.9. IR (KBr; cm^{-1}): 3441 (w), 3054 (w), 2957 (w), 1650 (vs), 1623 (w), 1594 (m), 1570 (m), 1462 (vs), 1434 (vs), 1422 (vs), 1388 (w), 1367 (m), 1320 (s), 1279 (m), 1224 (vs), 1150 (w), 1134 (m), 1074 (m), 1009 (w), 974 (m), 824 (m), 745 (vs). Anal. Calcd for $C_{20}H_{14}Cl_2N_4$ (381.26): C, 63.01; H, 3.70; N, 14.70. Found: C, 63.08; H, 3.75; N, 14.58.

(*E*)-2,6-Dibromo-*N*-(1-(6-(1*H*-benzo[*d*]imidazol-2-yl)pyridin-2-yl)ethylidene)benzenamine (L6). Using the same procedure as for the synthesis of **L5**, **L6** was obtained as a white powder in 28.5% yield. Mp: 113−114 °C. ^{1}H NMR (300 MHz, $CDCl_3$, TMS): δ 10.58 (brs, 1H, NH), 8.57(d, 1H, J = 7.8 Hz, Py), 8.46 (d, 1H, J = 7.8 Hz, Py), 8.00 (t, 1H, J = 7.9 Hz, Py), 7.89 (t, 1H, J = 5.0 Hz, Ar), 7.58 (m, 3H, Ar), 7.34 (m, 2H, Ar), 6.88 (t, 1H, J = 8.0 Hz, Ar), 2.40 (s, 3H, CH_3). ^{13}C NMR (75 MHz, $CDCl_3$, TMS): δ 170.5, 155.2, 150.6, 148.0, 147.5, 144.6, 138.1, 138.0, 133.9, 132.1, 129.2, 128.4, 125.6, 125.4, 124.3, 123.4, 123.1, 123.0, 120.4, 113.6, 111.4, 17.9. IR (KBr; cm^{-1}): 3405 (m), 3054 (m), 1648 (vs), 1620 (w), 1593 (m), 1569 (m), 1462 (s), 1422 (vs), 1389 (w), 1366 (m), 1318 (s), 1221 (vs), 1196 (w), 1149 (w), 1074 (m), 1008 (w), 993 (w), 822 (m), 756 (w), 742 (vs). Anal. Calcd for $C_{20}H_{14}Br_2N_4$ (470.16): C, 51.09; H, 3.00; N, 11.92. Found: C, 51.06; H, 3.04; N, 11.88.

4.4. Synthesis of Tridentate Iron Complexes Fe1−Fe6. The complexes **Fe1−Fe6** were synthesized by the reaction of $FeCl_2 \cdot 4H_2O$ with the corresponding ligands in ethanol. A typical synthetic procedure for **Fe1** can be described as follows: The ligand **L1** (71 mg, 0.21 mmol) and $FeCl_2 \cdot 4H_2O$ (79.5 mg, 0.20 mmol) were added to a Schlenk tube, followed by the addition of freshly distilled ethanol (5 mL) with rapid stirring at room temperature. The solution turned green immediately, and a blue precipitate was formed. The reaction mixture was stirred for 12 h, and then the precipitate was washed with diethyl ether twice and dried to give the pure product as a blue powder in 87.5% yield. IR (KBr; cm^{-1}): 3449 (m), 3065 (m), 2951 (w), 2915 (w), 1599 (vs), 1496 (m), 1473 (s), 1418 (s), 1374 (m), 1321 (s), 1274 (m), 1210 (s), 1098 (m), 1020 (w), 812 (m), 793 (w), 766 (m), 746 (s). Anal. Calcd for $C_{22}H_{20}Cl_2FeN_4$ (467.17): C, 55.56; H, 4.32; N, 11.99. Found: C, 55.50; H, 4.38; N, 11.87. Data for **Fe2** are as follows. Yield: 96.3%. IR (KBr; cm^{-1}): 3433 (m), 3066 (w), 2967 (m), 2934 (w), 1598 (vs), 1495 (w), 1475 (m), 1443 (w), 1413 (m), 1374 (m), 1321 (s), 1299 (m), 1273 (m), 1234 (w) 1202 (m), 1162 (w), 1116 (w), 812 (s), 791 (s), 766 (m), 755 (vs). Anal. Calcd for $C_{24}H_{24}Cl_2FeN_4$ (495.23): C, 58.21; H, 4.88; N, 11.31. Found: C, 58.15; H, 4.95; N, 11.28. Data for **Fe3** are as follows. Yield: 92.7%. IR (KBr; cm^{-1}): 3367 (w), 3061 (m), 2962 (s), 1595 (vs), 1496 (w), 1475 (m), 1439 (m), 1411 (s), 1370 (m), 1318 (vs), 1299 (m), 1273 (w), 1234 (w), 1200 (m), 1176 (w), 1130 (w), 1017 (w), 814 (m), 790

(m), 750 (vs). Anal. Calcd for $C_{26}H_{28}Cl_2FeN_4$ (523.28): C, 59.68; H, 5.39; N, 10.71. Found: C, 59.63; H, 5.50; N, 10.63. Data for **Fe4** are as follows. Yield: 85.0%. IR (KBr; cm^{-1}): 3415 (m), 3093 (m), 3062 (m), 2951 (m), 2917 (m), 1597 (vs), 1476 (vs), 1437 (m), 1416 (vs), 1371 (m), 1318 (s), 1298 (m), 1273 (m), 1217 (vs), 1152 (m), 1037 (w), 977 (w), 853 (s), 814 (s), 766 (m), 748 (vs). Anal. Calcd for $C_{23}H_{22}Cl_2FeN_4$ (481.2): C, 57.41; H, 4.61; N, 11.64. Found: C, 57.37; H, 4.65; N, 11.63. Data for **Fe5** are as follows. Yield: 82.7%. IR (KBr; cm^{-1}): 3433 (m), 3097 (w), 3058 (m), 1598 (vs), 1572 (w), 1476 (w), 1435 (vs), 1369 (m), 1327 (m), 1274 (m), 1224 (m), 1192 (w), 1150 (w), 1098 (w), 1018 (w), 856 (w), 813 (s), 791 (vs), 755 (vs). Anal. Calcd for $C_{20}H_{14}Cl_4FeN_4$ (508.01): C, 47.29; H, 2.78; N, 11.03. Found: C, 47.33; H, 2.82; N, 10.96. Data for **Fe6** are as follows. Yield: 84.3%. IR (KBr; cm^{-1}): 3427 (w), 3093 (w), 3060 (m), 2916 (w), 1597 (vs), 1572 (w), 1550 (m), 1495 (w), 1475 (m), 1426 (vs), 1368 (m), 1325 (m), 1298 (m), 1223 (m), 1192 (w), 1131 (w), 812 (m), 783 (m), 765 (m), 754 (s). Anal. Calcd for $C_{20}H_{14}Br_2Cl_2FeN_4$ (596.93): C, 40.24; H, 2.36; N, 9.39. Found: C, 40.15; H, 2.41; N, 9.32.

4.5. Synthesis of Tridentate Cobalt Complexes Co1−Co6. Complexes **Co1−Co6** were prepared by the same synthetic procedures and were obtained as green powders. The synthetic procedure of **Co1** can be described as follows: To a mixture of ligand **L1** (71 mg, 0.21 mmol) and $CoCl_2$ (26 mg, 0.20 mmol) was added ethanol (5 mL) at room temperature. The solution turned green immediately. The reaction mixture was stirred for 12 h, and the precipitate was collected by filtration and washed with diethyl ether, followed by drying under vacuum. The desired complex was obtained as a green powder in 78.5% yield. IR (KBr; cm^{-1}): 3432 (m), 3060 (w), 2961 (w), 1600 (vs), 1475 (s), 1417 (vs), 1373 (w), 1318 (m), 1210 (s), 1022 (w), 812 (m), 793 (w), 766 (m), 750 (vs). Anal. Calcd for $C_{22}H_{20}Cl_2CoN_4$ (470.26): C, 56.19; H, 4.29; N, 11.91. Found: C, 56.14; H, 4.34; N, 11.88. Data for **Co2** are as follows. Yield: 77.8%. IR (KBr; cm^{-1}): 3433 (m), 3064 (m), 2966 (s), 2934 (w), 1598 (vs), 1571 (w), 1495 (w), 1476 (m), 1414 (s), 1374 (s), 1321 (s), 1299 (m), 1272 (m), 1236 (w), 1201 (m), 1116 (w), 1023 (m), 978 (w), 854 (w), 812 (s), 791 (s), 750 (vs). Anal. Calcd for $C_{24}H_{24}Cl_2CoN_4$ (498.31): C, 57.85; H, 4.85; N, 11.24. Found: C, 57.81; H, 4.89; N, 11.18. Data for **Co3** are as follows. Yield: 82.3%. IR (KBr; cm^{-1}): 3406 (w), 3061 (w), 2964 (s), 1597 (s), 1572 (w), 1496 (w), 1476 (m), 1439 (w), 1412 (m), 1370 (m), 1319 (s), 1300 (m), 1272 (w), 1200 (m), 1129 (w), 1022 (w), 938 (w), 815 (m), 789 (m), 750 (vs). Anal. Calcd for $C_{26}H_{28}Cl_2CoN_4$ (526.37): C, 59.33; H, 5.36; N, 10.64. Found: C, 59.29; H, 5.41; N, 10.55. Data for **Co4** are as follows. Yield: 75.6%. IR (KBr; cm^{-1}): 3443 (m), 3058 (m), 2952 (w), 2915 (m), 1598 (vs), 1476 (s), 1437 (w), 1414 (s), 1370 (m), 1318 (m), 1299 (w), 1217 (m), 1154 (m), 1023 (w), 855 (m), 819 (w), 767 (w), 750 (vs). Anal. Calcd for $C_{23}H_{22}Cl_2CoN_4$ (484.29): C, 57.04; H, 4.58; N, 11.57. Found: C, 57.07; H, 4.64; N, 11.50. Data for **Co5** are as follows. Yield: 80.4%. IR (KBr; cm^{-1}): 3450 (m), 3059 (s), 2912 (w), 1626 (m), 1599 (vs), 1477 (m), 1436 (vs), 1417 (m), 1371 (m), 1320 (m), 1299 (m), 1275 (m), 1231 (m), 1197 (w), 1150 (w), 1094 (w), 1023 (w), 856 (w), 819 (m), 768 (m), 749 (vs). Anal. Calcd for $C_{20}H_{14}Cl_4CoN_4$ (511.1): C, 47.00; H, 2.76; N, 10.96. Found: C, 46.92; H, 2.80; N, 10.89. Data for **Co6** are as follows. Yield: 73.8%. IR (KBr; cm^{-1}): 3434 (m), 3057 (s), 2911 (w), 1626 (w), 1598 (vs), 1549 (m), 1478 (m), 1428 (vs), 1416 (s), 1371 (m), 1321 (m), 1298 (m), 1273 (m), 1227 (m), 1093 (w), 1024 (w), 817 (m), 766 (m), 749 (s). Anal. Calcd for $C_{20}H_{14}Br_2Cl_2CoN_4$ (600.02): C, 40.04; H, 2.35; N, 9.34. Found: C, 39.98; H, 2.39; N, 9.28.

4.6. Procedure for Ethylene Oligomerization and Polymerization. The catalyst precursor was transferred to the fully dried reactor containing100 mL of toluene under nitrogen atmosphere. The required amount of cocatalyst was then injected into the reactor via a syringe. At the reaction temperature, the reactor was sealed and pressurized to high ethylene pressure, and the ethylene pressure was maintained with the ethylene feed. After the reaction mixture was stirred for the desired time, the pressure was released and a small amount of the reaction solution was collected, which was then analyzed by gas chromatography (GC) to determine the composition and mass distribution of oligomers obtained. Then the residual reaction solution was quenched with 5% hydrochloric acid in ethanol. The precipitated polyethylene was collected by filtration, washed with ethanol and water, and dried under vacuum to constant weight.

4.7. X-ray Crystallographic Studies. The single-crystal X-ray diffraction studies for **Fe3**, **Co2**, and **Co4** were carried out on a Rigaku RAXIS Rapid IP diffractometer with graphite-monochromated Mo Kα radiation ($\lambda = 0.71073$ Å). Cell parameters were obtained by global refinement of the positions of all collected reflections. Intensities were corrected for Lorentz and polarization effects and empirical absorption. The structures were solved by direct methods and refined by full-matrix least-squares on F^2. All non-hydrogen atoms were refined anisotropically, and all hydrogen atoms were placed in calculated positions. Structure solution and refinement were performed by using the SHELXL-97 package.[50] Crystal data and processing parameters for **Fe3**, **Co2**, and **Co4** are available in the Supporting Information.

Acknowledgment. This work was supported by NSFC No. 20674089 and 20621091. We are grateful to Dr. Mark Schormann for his kindness in proofreading the manuscript.

Supporting Information Available: Crystal data and processing parameters for **Fe3**, **Co2**, and **Co4** and CIF files giving crystallographic data for **Fe3**, **Co2**, and **Co4**. This material is available free of charge via the Internet at http://pubs.acs.org.

OM801141N

(50) Sheldrick, G. M. *SHELXTL-97, Program for the Refinement of Crystal Structures*; University of Göttingen: Göttingen, Germany, 1997.